SUPERLATTICE CASCADE SOLAR CELL

M.W. Wanlass and A.E. Blakeslee

Solar Energy Research Institute
Golden, Colorado 80401

ABSTRACT

This paper reports progress toward realization of a new cascade solar cell structure whose chief advantages over other present concepts are: use of silicon for the substrate and low bandgap cell; avoidance of the necessity of lattice matching; and incorporation of a GaAs/GaP superlattice to enhance efficiency and provide a low-resistance connecting junction. Details of the design and operation of an OMCVD system for growing this structure are presented. Results of experiments to optimize layer thickness, compositional uniformity, and surface morphology are described.

INTRODUCTION

Various analyses of the economics of photovoltaic conversion processes point out that practical use of solar electric power on a commercial scale in the coming decades will demand significant increases in the efficiency of available photovoltaic cells (1,2). This requirement dictates that a more complete utilization of the incident solar spectrum be achieved than is possible with any single junction device, i.e., that the potential of multijunction solar cells to yield conversion efficiencies in the 30 - 40% range (3) must be realized.

To reach this goal, it is necessary to find adequate solutions to the two major impediments in present-day cascade cell technology: the lattice mismatch problem and the connecting junction problem. The former problem occurs because no pair of atomic or binary compound semiconductors having the proper bandgap values to yield the highest efficiency have similar lattice constants as well. The lattice mismatch causes large numbers of lattice defects, primarily misfit dislocations, to arise during multilayer crystal growth. Excessive numbers of these defects will obviously be detrimental to the efficiency of the top cell, although what the tolerable limit in dislocation density is has not yet been determined. The interconnect problem occurs because, since the two active p-n junctions have the same polarity, there is an intervening junction of the opposite polarity which must drop negligible voltage in order to minimize internal power loss. Present attempts to provide this low resistance connection include use of a forward-biased tunnel junction (4) and actually shorting out the reverse polarity junction with metal stripes (5), but neither of these approaches is technologically very desirable. This paper describes a novel cascade solar cell whose key feature, a superlattice, is expected to provide a simultaneous solution to both the mismatch and the interconnect problems.

DEVICE CONCEPT

The idea of using a superlattice to solve the mismatch and interconnect problems has been set out in detail in a recent patent (6). The method is applicable in principle to a wide variety of high-low bandgap cascade devices and indeed to many device structures other than solar cells, but in the present instance the discussion will be limited to the particular cascade cell scheme shown in Fig. 1. It is a multilayer structure grown by organometallic chemical vapor deposition (OMCVD) and consists of the following essential parts:

a) low-cost silicon substrate and low bandgap cell (E_g=1.1 eV);
b) thin GaP layer lattice-matched to the Si;
c) graded alloy region of $GaAs_{1-x}P_x$ from x=1 to x=.3;
d) constant composition layer of $GaAs_{.7}P_{.3}$;
e) GaAs/GaP superlattice;
f) top cell region of $GaAs_{.7}P_{.3}$ (E_g=1.8 eV).

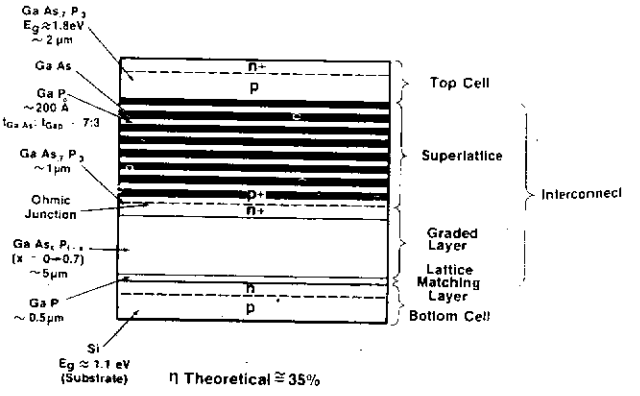

Figure 1. Device structure.

0160-8371/82/0000-0584 $00.75

Although calculations have indicated that the very highest efficiency would result from 0.95 and 1.65 eV cells in tandem (3), the calculated maximum is a very broad one, and the pair chosen here (1.1 and 1.8 eV) should serve almost as well. Two significant technological advantages justify our choice: the low cost and ready availability of silicon, and the shorter range of graded composition consistent with the higher bandgap upper cell. Fine tuning of the efficiency in accordance with variable operating parameters can easily be accomplished by altering the amount of compositional grading.

A superlattice is a thin (~1μm) semiconductor structure comprised of many ultrathin layers (~100Å each) of two different semiconductors alternating with one another. It exhibits properties which tend to be intermediate between those of the two constituent materials but may be somewhat different from either one. It offers the possibility of creating semiconductors with made-to-order properties such as the bandgap or optical absorption coefficient. It was first proposed by Esaki and Tsu (7) in 1970 as a quantum mechanical curiosity with a potential for very high frequency response. Several device proposals based on the superlattice concept have followed (8, 9).

The function of the superlattice in the proposed tandem solar cell is not, however, as a new photoelectric conversion material but rather as a layer which can filter out or block dislocations. Matthews and Blakeslee (10) have demonstrated that growth of a superlattice layer following the compositionally graded layer serves to confine all the dislocation lines in planes normal to the growth direction so that they do not propagate into the active solar cell region. They were able to reduce the dislocation density in a $GaAs/GaAs_{.5}P_{.5}$ superlattice from 10^8 per cm^2 to almost zero. Producing a similar effect in our tandem cell should significantly improve the efficiency of the upper cell and, therefore, that of the cell as a whole.

When operating properly, the mechanism transforms the threading dislocations into misfit dislocations which are confined to the first few interfaces of the superlattice. The density of dislocations at the beginning of the superlattice is, therefore, extremely high (and virtually zero thereafter). If the reversing p-n junction is placed at precisely that point, it is expected that the dislocations would at least partially, if not totally, short it out, as predicted by James (11). If in addition, the doping is made very high and abrupt on both sides of this junction in order to enhance the probability of tunneling, it is likely that the junction will have a very low resistance and thus provide a satisfactory interconnect.

To construct the cascade cell described here is a formidable task, imposing severe demands upon crystal growth and device fabrication techniques. Foremost are the two important conditions explicit in the prescription for successful dislocation elimination (10). In order for the mechanism to operate properly, the sublayers in the superlattice must have a thickness less than the critical thickness for creation of new dislocations (estimated to be in the neighborhood of 300Å), and the misfit between the superlattice taken as a whole and the underlying constant composition $GaAs_{1-x}P_x$ layer must be close to zero. If these two conditions are not satisfied, then it is likely that the uncompensated strain in the superlattice will result in an increase rather than a decrease in the dislocation density. This is indeed what happened during the growth of the first superlattice crystals when a graded layer was not incorporated in the structure (12).

In our present case, where the underlayer has the composition $GaAs_{.7}P_{.3}$, the second condition is met by adjusting the composition of the superlattice to be on the average 70% GaAs - 30%GaP. This could be done by growing sublayers of equal thickness but different composition, e.g. GaAs and $GaAs_{.4}P_{.6}$, but we have chosen to make the superlattice out of alternating layers of pure GaAs or GaP and vary their thicknesses in the ratio of 7:3.

In addition to the necessity for close compositional matching, a number of other requirements must be satisfied in order to achieve the ultimate goal of a high efficiency cascade cell. For good performance, the structure must show low electrical series resistance and have high optical transparency except in the junction areas. To what extent these characteristics are exhibited can be determined only when the structure is built. To be economically feasible, it should consist of only a few microns of expensive Ga-containing material atop the relatively inexpensive Si substrate. The minimum thickness of graded layer and the minimum number of superlattice sublayers necessary for a successful device can also be determined only by experiment. To grow large-area structures and keep the various layer thicknesses uniform throughout is a challenging problem in gas dynamics. Accurate placement of a p-n junction within a few hundred angstroms of the bottom of the superlattice in order to take full advantage of the shorting effect of the dislocation pileup may be difficult. And finally, what may turn out to be the most serious problem of all is the growth of a sound epitaxial layer of GaP on the Si substrate. Heterepitaxy of GaP on Si by OMCVD has been demonstrated (13) but growth of a layer good enough to support all the subsequent layers and survive the thermal stresses to which it will be submitted is quite another matter.

Our experimental approach toward the solution of all these problems and progress made to date in that direction constitute the remainder of this paper.

EXPERIMENTAL

Gas Handling System

The equipment used to fabricate the cascade structure consists of a conventional OMCVD system coupled with a specially designed AsH_3/PH_3 gas handling system. The total system is depicted schematically in Fig. 2. The OMCVD portion of the system provides the input of trimethyl gallium (TMG), dopants, and H_2 carrier gas to the growth reactor. The AsH_3/PH_3 system is a fully automated subsystem for manipulation of the input of AsH_3 and/or PH_3 to the growth reactor. A simplified schematic of this subsystem is shown in Fig. 3. The AsH_3 and PH_3 flow rates are controlled by electronic mass flow controllers (MFC), and the gas flows can be directed either to vent or to the growth reactor by the actuation of pairs of pneumatically operated bellows valves (one normally open, one normally closed). Gases directed to the growth reactor travel down a narrow injector tube and exit just above the substrate to mix with the TMG, dopant, and H_2 carrier ambient, as indicated in Fig. 3. With this system, either a $GaAs_{1-x}P_x$ layer having any desired value of x or a superlattice can be deposited whenever desired. Hence, the entire cascade structure or, indeed, structures of considerably greater complexity, can be grown in a continuous fashion.

For example, during the growth of the graded layer both the AsH_3 and PH_3 are switched to the growth reactor and the respective mass flow controller flow rates are automatically varied to produce a linear gradation in $GaAs_{1-x}P_x$ across the layer. In contrast, the growth of the superlattice involves switching constant flow rates of AsH_3 and PH_3 alternately between growth reactor and vent such that pure pulses of first AsH_3 and then PH_3 travel down the injector tube, and individual layers of GaAs and GaP are

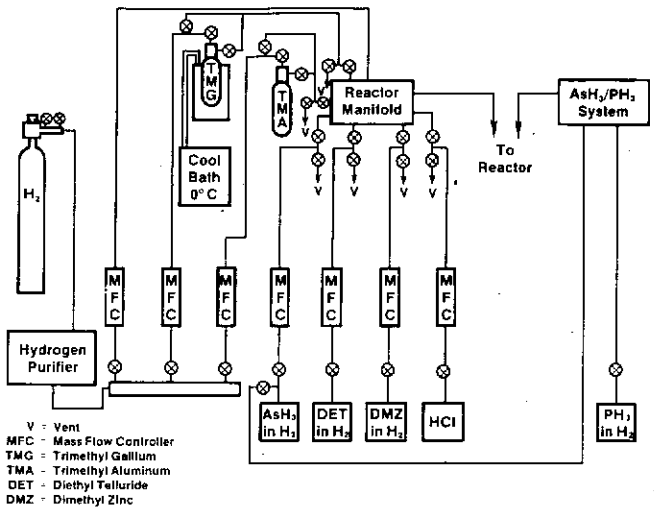

Figure 2. OMCVD crystal growth system.

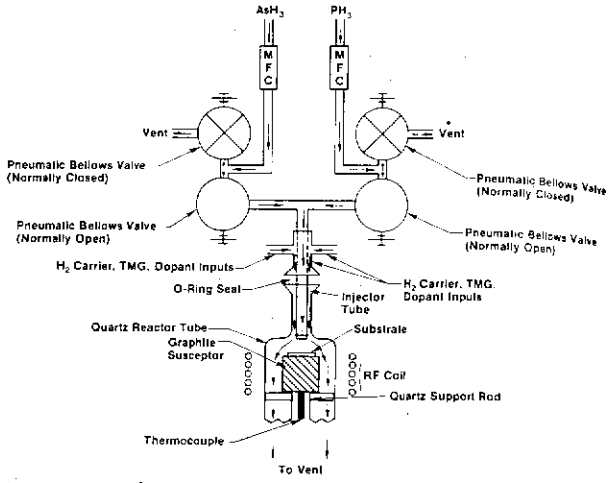

Figure 3. Details of the AsH_3/PH_3 system and the reactor zone.

deposited. The average composition of the superlattice is controlled by varying the thickness of the individual GaAs and GaP layers. Automatic control of the valve switching provides a resolution of 0.1 s in the AsH_3/PH_3 pulse duration, corresponds to a transition region of ~5Å in the absence of any gaseous interdiffusion.

Reactor Design

In order to grow the cascade structure in one continuous process, careful design and construction of the gas system and growth reactor was found to be necessary. In the growth reactor, adequate mixing of the various gases and uniform flux delivery are essential for uniform composition and growth rate. However, the system must also be capable of delivering individual pulses of AsH_3 and PH_3 for the superlattice. Mixing of the AsH_3 and PH_3 pulses prior to deposition is undesirable at this stage, since sharp compositional gradients within the superlattice are essential to its function. Several modifications were made to the original design in order to properly fulfill requirements.

Figure 4 portrays the evolution of the reactor zone, which includes the upper portion of the growth reactor, the injector tube, and the susceptor. Compositional and growth rate uniformity depend strongly on the velocity distribution and the flux density of the gases within the reactor zone, both of which, in turn, are determined by the geometry of the reactor zone itself. The original reactor zone design shown in Fig. 4(a) yielded well-defined superlattice layers but gave poor surface morphology, compositional uniformity, and growth rate uniformity. The transitional design shown in Fig. 4(b) gave very uniform crystalline layers but was incapable of producing a well-defined superlattice due to AsH_3/PH_3 pulse mixing prior to growth. The design which satisfies all of the

requirements of the cascade structure is shown in Fig. 4(c) and is currently in use. This present system features radial injection of the AsH_3/PH_3 input from the bottom of the injector tube, which provides uniform distribution of the AsH_3/PH_3 mixture across the sample while maintaining well-defined superlattice layer growth during pulsing. Changing the shape of the top portion of the growth reactor, using a smaller diameter susceptor, and making adjustments in the H_2 carrier flow rate and growth rate were all found to improve the quality of grown layers.

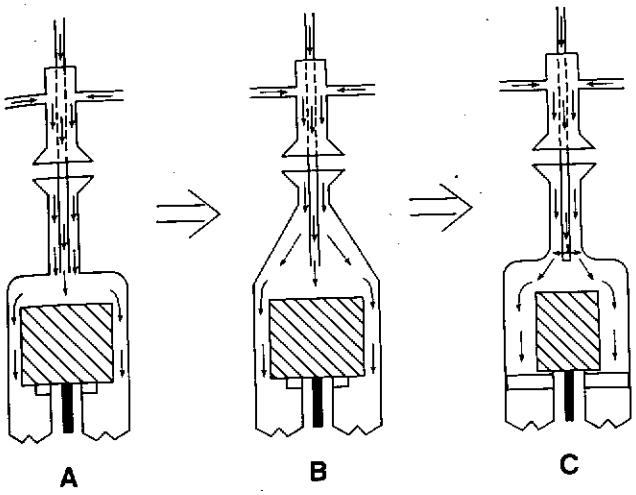

Results

	Design		
	A	B	C
Superlattice layer definition	Good	Poor	Good
Surface morphology	Poor	Good	Good
Compositional uniformity	Poor	Good	Good
Growth rate uniformity	Poor	Good	Good

Figure 4. Evolution of the reactor zone.

Procedure

Since the epitaxial growth of GaP on Si by OMCVD has been shown to be feasible but difficult (13), it was decided that the initial test structures for the purpose of demonstrating the concept would be grown on GaAs substrates and that the problem of growing GaP on Si would be addressed at a later date. The GaAs-based test structure offers all of the essential features of the structure shown in Fig. 1 and differs only in the inverted graded region necessary to accommodate the GaAs substrate. All of the structures mentioned in this report were grown on GaAs, but future plans include growing similar structures on GaP substrates.

Cr-doped, (100)-oriented GaAs substrates were degreased with conventional solvents and chemically etched to a depth of several microns with 3:1:1 $H_2SO_4:H_2O_2:H_2O$ at 20°C prior to insertion in the cleaned growth reactor. Crystalline layers were deposited at an average growth rate of 0.30 μm/min by passing a mixture of 10% AsH_3 and/or PH_3 in H_2, TMG, and 2000 ccm of H_2 over the substrate at 750°C. Typical AsH_3 and PH_3 flow rates ranged from 100 to 200 ccm with an overall V/III ratio greater than 20. Growth of doped layers was accomplished by metering very small flows of dimethyl zinc or diethyl telluride, each 100 ppm in H_2, for p- or n-type, respectively.

RESULTS

The bulk of the measurements performed to date have been dimensional and compositional in nature. In order to properly characterize the superlattice, its layer thickness, compositional variation, and average composition must all be considered. Figure 5 shows two superlattice samples which were cleaved, treated with a delineation etch, and photographed using scanning electron microscopy(SEM). The AsH_3 and PH_3 pulse times were equal in both cases, but differed by a factor of three between the samples. Otherwise, the samples were grown under the same conditions. Since growth rate in OMCVD systems is Group III mass transport limited and the TMG flux is held constant, the GaAs/GaP average layer thickness should be proportional to the AsH_3/PH_3 pulse time. It is seen that this proportionality is borne out in the example of Fig. 5. The layers are not absolutely planar, but although near-perfect layer planarity is necessary for superlattices used in electronic applications, the layer integrity displayed in our samples should be of sufficient quality to provide effective dislocation filtering.

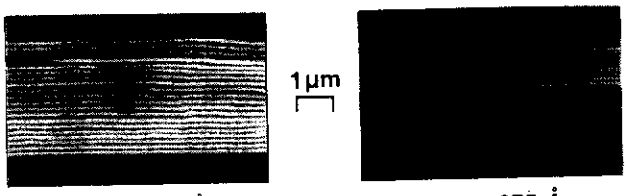

Figure 5. Scanning electron micrograph of superlattice showing average layer thickness proportional to pulse time.

A qualitative composition profile of the superlattice obtained with the ion microprobe is given in Fig. 6. Reasonably sharp composition gradients between adjacent GaAs and GaP layers are suggested by this data. However, a large deviation from the expected average composition has been found. It was initially assumed that superlattice regions with an average composition of $GaAs_{.7}P_{.3}$ could be grown by simply injecting the AsH_3 and PH_3 with a 7:3 ratio in the pulse

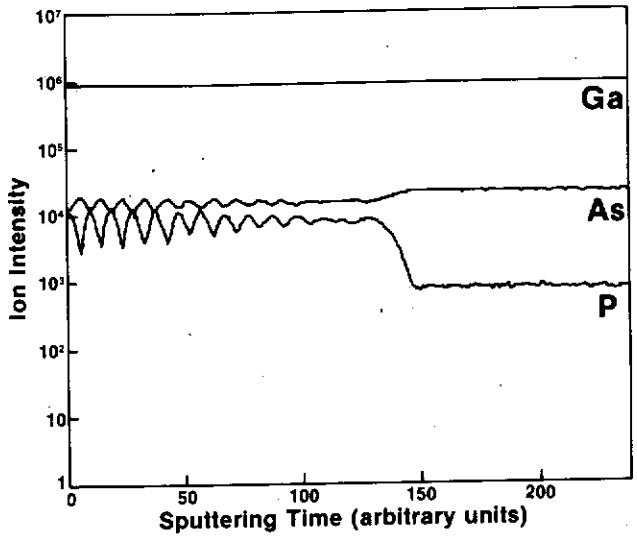

Figure 6. Ion Probe SIMS depth profile of superlattice revealing periodic variations in the arsenic and phosphorus content.

times. However, electron probe microanalysis (EPMA) of superlattice samples produced in this manner has shown them to be consistently P-deficient. We believe this effect to be caused by overlap or partial mixing of the AsH_3/PH_3 pulses prior to deposition combined with inefficient decomposition of PH_3 in the presence of AsH_3 (14). An obvious solution to this problem, which is being undertaken, is to increase the PH_3 pulse time until the desired average composition is achieved.

Another serious problem affecting the matching of composition necessary for dislocation removal was revealed by EPMA of early $GaAs_{1-x}P_x$ layers. It was found that the PH_3/AsH_3 flow rate ratio in the vapor was always much higher than the resultant P/As atomic ratio in the grown solid due to inefficient decomposition of the PH_3 at the growth temperature. A

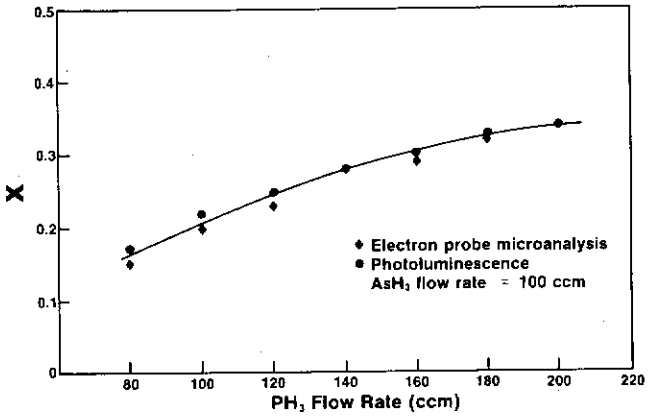

Figure 7. OMCVD $GaAs_{1-x}P_x$ composition calibration.

series of $GaAs_{1-x}P_x$ films was grown to determine the x-value dependence on the PH_3 input flow rate. The compositions of the films were measured using both EPMA and photoluminescence techniques as displayed in Fig. 7. As expected, the $GaAs_{1-x}P_x$ x-value increased with increasing PH_3 input and a PH_3/AsH_3 flowrate ratio of ~1.55 gave the desired top cell material composition of $GaAs_{.7}P_{.3}$.

During the course of this work, a variety of surface conditions has been observed on the grown samples. Early samples were characterized by several surface conditions existing on the same sample, including a central region composed of liquid Ga droplets and VLS whisker growth (15) and outer regions of single crystal growth with various surface textures. Modifications to the apparatus and growth techniques have resulted in improvements to the surface morphology. Recent samples have very uniform surfaces but exhibit the familiar orthogonal cross-hatch characteristic of mismatched layers grown on the (100) face. Top cell layers with acceptable growth rate and compositional uniformity and with an average composition of $GaAs_{.7}P_{.3}$ can now be reproducibly grown. A cross-section of our entire cascade structure grown without proper composition matching is pictured in Fig. 8.

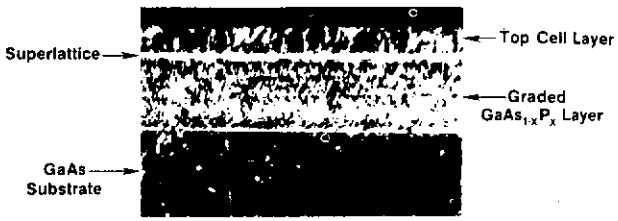

Figure 8. Complete test structure grown on (100) GaAs substrate.

Due to the lack of control of the average composition of the superlattice, complete test structures with proper composition matching have not yet been produced, precluding the acquisition of meaningful electrical data. It is planned that a shallow homojunction solar cell, similar to those already fabricated by Fan et al (16) and Fraas (17), will be used for the $GaAs_{.7}P_{.3}$ top cell. Shallow homojunction cells in OMCVD GaAs have already been produced with V_{oc}=0.87 V, J_{sc}=13.3 mA/cm^2, FF=0.73, and η=8.4% (1Sun, AM1), which should improve as the p-n junction depth is optimized.

ACKNOWLEDGMENT

We wish to thank our many colleagues at SERI who have contributed to this work, expecially P.E. Russell for the ion microprobe analysis, C.R. Harrington for the electron probe analysis, and R.J. Matson for the scanning electron microprobe. Without the early cooperation of K.W. Mitchell in formulating the superlattice cascade concept, the project would never have come into being. This work was performed under DOE contract No. EG-77-C01-4042.

REFERENCES

1. D.L. Bowler and M. Wolf, IEEE Trans. on Components, Hybrids, and Manufacturing Technology, CHMT-3, 464 (1980).

2. R.W. Taylor, Proc. Electrochem. Soc. Symp. on Materials and New Processing Technologies for Photovoltaics, Montreal, May 9-14, 1982.

3. K.W. Mitchell, Proc. International Electron Device Meeting, Washington, D.C., December 1978, pp. 254-257; Proc. 15th IEEE Photovoltaics Specialists Conf. (1981), pp. 142-146.

4. S.M. Bedair, J. Appl. Phys., 50 7167 (1979).

5. P. Borden, R. LaRue, M. Ludowise, P. Gregory, and R. Sazena, DM Tech. Digest, 81CH1708-7 150 (1981).

6. A.E. Blakeslee and K.W. Mitchell, U.S. Patent 4,278,474.

7. L. Esaki and R. Tsu, IBM J. Res. Develop., 14 61 (1970).

8. G.H. Dohler, J. Vac. Sci. Technol. 16 851 (1979).

9. M.D. Camras, N. Holonyak, Jr., K. Hess, J.J. Coleman, R.D. Burnham, and D.R. Scifres, Appl. Phys. Lett., 41 317 (1982).

10. J.W. Matthews and A.E. Blakeslee, J. Cryst. Growth, 32, 265 (1976).

11. L.W. James, U.S. Patent 4,017,332.

12. J.W. Matthews and A.E. Blakeslee, J. Cryst. Growth, 27, 118 (1974).

13. H.B. Pogge, B.M. Kemlage and R.W. Broadie, J. Cryst. Growth, 37 (1977).

14. V.S. Ban, J. Electrochem. Soc., 118, 1473 (1971).

15. R.S. Wagner and W.C. Ellis, Appl. Phys. Lett., 4 89 (1964).

16. J.C.C. Fan, C.O. Bozler, and R.L. Chapman, Appl. Phys. Lett., 32 390 (1978).

17. L.M. Fraas, in Proc. SPIE, Vol. 323, "Semiconductor Growth Technology".